



California State University, San Bernardino
CSUSB ScholarWorks

Electronic Theses, Projects, and Dissertations

Office of Graduate Studies

9-2020

Tile Based Self-Assembly of the Rook's Graph

Ernesto Gonzalez

Follow this and additional works at: <https://scholarworks.lib.csusb.edu/etd>



Part of the [Other Mathematics Commons](#)

Recommended Citation

Gonzalez, Ernesto, "Tile Based Self-Assembly of the Rook's Graph" (2020). *Electronic Theses, Projects, and Dissertations*. 1085.

<https://scholarworks.lib.csusb.edu/etd/1085>

This Thesis is brought to you for free and open access by the Office of Graduate Studies at CSUSB ScholarWorks. It has been accepted for inclusion in Electronic Theses, Projects, and Dissertations by an authorized administrator of CSUSB ScholarWorks. For more information, please contact scholarworks@csusb.edu.

TILE BASED SELF-ASSEMBLY OF THE ROOK'S GRAPH

A Thesis

Presented to the

Faculty of

California State University,

San Bernardino

In Partial Fulfillment

of the Requirements for the Degree

Master of Arts

in

Mathematics

by

Ernesto Gonzalez

June 2020

TILE BASED SELF-ASSEMBLY OF THE ROOK'S GRAPH

A Thesis

Presented to the

Faculty of

California State University,

San Bernardino

by

Ernesto Gonzalez

June 2020

Approved by:

Cory Johnson, Committee Chair

Rolland Trapp, Committee Member

Jeffrey Meyer, Committee Member

David Maynard, Chair, Department of Mathematics

Corey Dunn, Graduate Coordinator

ABSTRACT

The properties of DNA make it a useful tool for designing self-assembling nanostructures. Branched junction molecules provide the molecular building blocks for creating target complexes. We model the underlying structure of a DNA complex with a graph and we use tools from linear algebra to optimize the self-assembling process. Some standard classes of graphs have been studied in the context of DNA self-assembly, but there are many open questions about other families of graphs. In this work, we study the rook's graph and its related design strategies.

ACKNOWLEDGEMENTS

In my mathematical career I have had two great teachers that have helped out tremendously in my learning. I'd like to thank Theresa Hert, which was the first teacher to hook me onto mathematics. If it wasn't for Mrs. Hert, I would have never found out what my gift was and I would have never thought of pursuing a degree in mathematics. Thank you Mrs. Hert for your indirect contribution to my thesis. The other great teacher that has made a difference in my learning, I had in my first quarter at Cal State San Bernardino. Ever since that quarter, I made the effort to take as many classes as I could with her. Dr. Johnson, thank you for being a great instructor!!! Dr. Johnson helped me tremendously with my learning and as my committee chair. Your help in my thesis is greatly appreciated and it has been a delight seeing my thesis evolve into an elegant piece of work. Lastly, I'd like to thank my parents Ted and Emma Gonzalez. My parents both put a big value on getting an education and pushed me to achieve more than the bare minimum. Thank you mom and dad for always believing in me, pushing me to try to be the best and thank you for all the financial and moral support.

Table of Contents

Abstract	iii
Acknowledgements	iv
List of Figures	vi
1 Introduction	1
1.1 Introduction	1
1.2 Graph Theory of the Rook's Graph	1
1.3 DNA Self-Assembly	3
1.4 Goal for the Project	6
2 Necessary Information About DNA Self-Assembly	7
2.1 Background Information	7
2.2 Information for Scenario 1	9
2.3 Information for Scenario 2	10
3 Rooks Graph Under Scenario 1	12
3.1 Method Used for the Construction	12
3.2 $n \times n$ Rook's Graph	12
3.3 $m \times n$ Rook's Graph	14
4 Rook's Graph Under Scenario 2	16
4.1 $2 \times n$ Rook's Graph.	16
4.2 $m \times n$ Rook's Graph	23
4.3 $n \times n$ Rook's Graph	25
5 Conclusion	28
Bibliography	29

List of Figures

1.1	Examples of rook's graphs	2
1.2	DNA double helix	3
1.3	Complete graph K_3	5
3.1	3×3 rook's graph in Scenario 1	13
3.2	2×4 rook's graph in Scenario 1	15
4.1	Complete graph K_5 and an isomorphic copy	18
4.2	Making a rook's graph from two complete graphs	18
4.3	2×3 rook's graph	19
4.4	Lattice points	21
4.5	2×4 rook's graph	22
4.6	3×4 rook's graph	24
4.7	3×3 rook's graph	25
4.8	4×4 rook's graph	26

Chapter 1

Introduction

1.1 Introduction

The Watson-Crick complementary properties of DNA strands make self-assembly an interesting technique for building structures at the nanoscale [EMJP19, See07, See82]. Applications of DNA self-assembly include, but are not limited to, drug delivery, biosensors, biomolecular computing, and nanorobotics [EMPB⁺14]. Furthermore, an essential step in building the self-assembling nanostructures is designing the component molecular building blocks. These design strategy problems fall naturally into the realm of graph theory [EMP11]. In addition to the practical applications of DNA self-assembly, there is interest in expanding the theory around design strategies. This research focuses on modeling the self-assembly of a structure isomorphic to a rook's graph and related design questions. The rest of Chapter 1 includes an introduction to the graph theoretical properties of the rook's graph, followed by an introduction to the mathematical abstraction of DNA self-assembly. We conclude the chapter with specific goals of this project.

1.2 Graph Theory of the Rook's Graph

This project studies the tile based DNA self-assembly of the rook's graph. To begin, note that the rook's graph is a graph that represents all the legal moves that the rook chess piece can make on an $m \times n$ chessboard where m and n need not be distinct. That is, the squares of the chessboard represent the vertices on a graph, and all the legal moves that the rook's piece can make will produce an edge. For example, Figure 1.1a is a

3×3 rook's graph and Figure 1.1b is a 2×6 rook's graph. Recall that a *graph* G consists of a set $V = V(G)$ of vertices, a set $E = E(G)$ of edges, and a map $\mu : E \rightarrow V^{(2)}$ where $V^{(2)}$ is the set of unordered pairs of elements of V . Furthermore, if $\mu(e) = \{u, v\}$, then u and v are the vertices incident with e . Additionally, (u, e) is a *half edge* of G if $v \in \mu(e)$, and H denotes the set of half edges of G [EMJP19]. Here are some graph theoretical properties of the rook's graph in order to understand it better. First, the rook's graph is a regular graph. That is, every vertex of the graph has the same degree; specifically, the degree of each vertex is $(m - 1) + (n - 1)$. Another property of the rook's graph is that it is the Cartesian product of two complete graphs of order m and n . For two graphs G and H , the *Cartesian product* $G \times H$ has vertex set $V(G \times H) = V(G) \times V(H)$. That is, every vertex of $G \times H$ is an ordered pair (u, v) , where $u \in V(G)$ and $v \in V(H)$. Two distinct vertices (u, v) and (x, y) are adjacent in $G \times H$ if either (1) $u = x$ and $vy \in E(H)$ or (2) $v = y$ and $ux \in E(G)$ [CZ12]. One can conclude that an $m \times n$ rook's graph is $K_m \times K_n$ where K_m and K_n are complete graphs with m vertices and n vertices respectively.

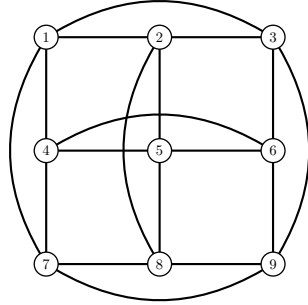
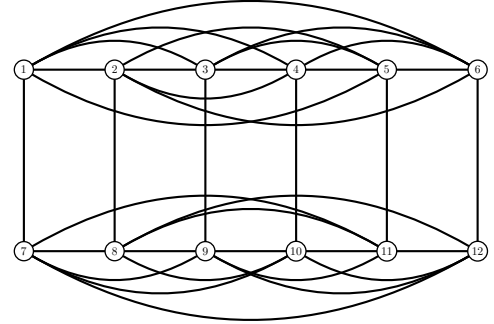
(a) 3×3 rook's graph(b) 2×6 rook's graph

Figure 1.1: Examples of rook's graphs

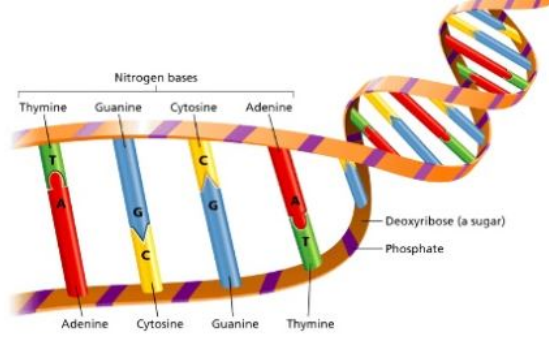


Figure 1.2: DNA double helix

1.3 DNA Self-Assembly

Recall, DNA is a ladder shaped molecule that is twisted into a shape that is known as a double helix. The “rungs” of this ladder-looking molecule are composed of two nitrogen bases. These bases are called adenine(A), thymine(T), guanine(G) and cytosine(C), and they bond together in a particular manner. That is, (A) pairs with (T) and (C) pairs with (G), see Figure 1.2. This property of DNA is used to design structures that will self-assemble. The building blocks of DNA self-assembly are k -armed branched junction molecules. These molecules are “spider” shaped in which its “body” represents a vertex of the target structure, and its k -arms are double strands of DNA in which one strand extends further than the other. The longer strand forms a **cohesive-end** at the end of the arm that can only bond to another cohesive-end with complementary bases. The bonded cohesive-ends form the edges of the DNA complex. The DNA complex is complete if it has no unmatched cohesive-ends. The k -armed branched junction molecules with cohesive-ends are modeled by a k -degree vertex with k incident half-edges [EMP11, EMJP19]. The following definition from [EMJP19] is the mathematical formalism that will be used to study these objects.

Definition 1.1. *The combinatorial objects for tile-based assembly design are as follows:*

- **Cohesive-end type:** *Given a finite set of symbols Σ , called an alphabet, the extended cohesive-ends on the arms are denoted by an “unhatted” letter in Σ and its complement by the same letter, but “hatted”, that is $\hat{\Sigma} = \{\hat{x} \mid x \in \Sigma\}$.*

- **Bond-edge type:** A cohesive-end type joined to its complement forms a bond-edge type, which are identified by the unhatted letter label. For example, cohesive-ends a and \hat{a} will join to form a bond-edge of type a .
- **Tile:** The combinatorial abstraction of a branched junction molecule is called a tile. It consists of a vertex with half-edges labeled by the cohesive-end types on the arms of the molecule the tile represents, and is denoted by a multi-set of its cohesive-end types whose multiple entries of the same cohesive-end type are indicated by the exponent to the corresponding symbol.
- **Pot:** A pot is a collection of tiles such that for any cohesive-end type that appears on any tile in the pot, its complement also appears on some tile in the pot. A pot is a set $P = \{t_1, t_2, \dots, t_k\}$ where each t_i is a tile ($i = 1, \dots, k$) and for all $a \in \Sigma$, if there is an i such that $a \in t_i$, then there is a $j \in \{1, \dots, k\}$ such that $\hat{a} \in t_j$. The set of bond-edge types that appear in the tiles of P is denoted with $\Sigma(P)$, and define $\#P$ to be the number of distinct tile types in P .
- **Assembly design:** An assembly design is a labeling $\lambda : H \rightarrow \Sigma \cup \hat{\Sigma}$ of the half edges of a graph G with the elements of Σ and $\hat{\Sigma}$ such that if $e \in E(G)$ and $\mu(e) = \{u, v\}$, then $\widehat{\lambda(v, e)} = \lambda(u, e)$. This means that each edge receives both hatted and an unhatted symbol on its half edges. The convention that λ provides each edge with an orientation that starts from the unhatted half edge to the hatted half edge is used.
- The set of tiles associated with an assembly design λ of a graph G is the set $P_\lambda(G) = \{t_v \mid v \in V(G)\}$ where $t_v = \{\lambda(v, e) \mid v \in \mu(e), e \in E(G)\}$. This means that for each vertex v of G , the assembly design specifies a tile t_v whose multi-set is the set of labels of half edges incident to v . Expand the labeling λ to a labeling on vertices with $\lambda : V \rightarrow P_\lambda(G)$ such that $\lambda(v) = t_v$.

An example of a pot P that realizes the complete graph on three vertices K_3 , as in Figure 1.3, is $P = \{t_1 = \{a^2\}, t_2 = \{\hat{a}, b\}, t_3 = \{\hat{a}, \hat{b}\}\}$. This pot P has cohesive-end types a, \hat{a}, b, \hat{b} , with bond-edge types a, b . Notice that P is a pot since for each unhatted label in some tile, there exists another tile that has its complementary hatted label. According to [EMPB⁺14], when one requires a complex to be complete, “we may adopt the convention of orienting edges from unhatted cohesive-ends towards hatted cohesive-

ends”. Another convention that will be adopted in this paper, is giving each bond-edge type a different color for readability.

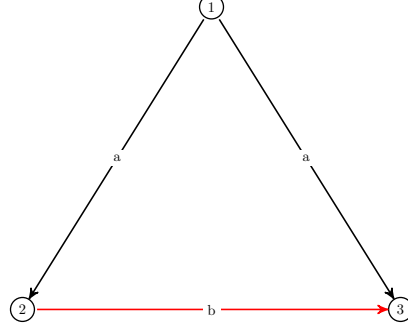


Figure 1.3: Complete graph K_3

Due to the cost of generating synthetic DNA, laboratories must be efficient in the design of self-assembling DNA. One translates the problem of efficiency into the following mathematical problem. Given a graph G , one wishes to know the minimum number of tile and bond-edge types that must be designed to construct the target complex. This question is considered under three different scenarios [EMPB⁺14]:

1. *Scenario 1.* The possibility that graphs with fewer vertices than the target graph may be created from the pot of tile types used to build the target graph is allowed.
2. *Scenario 2.* The possibility that graphs with the same number of vertices as, but not isomorphic to, the target graph may be created from the pot of tile types that builds the target graph. It is required that no complexes with fewer vertices can be created from the pot of tile types used to build the target graph.
3. *Scenario 3.* It is required that graphs with the same number of vertices must be isomorphic to the target graph.

Let $T_i(G)$ denote the minimum number of tile types needed to construct a graph G in Scenario i . Likewise, in Scenario i , let $B_i(G)$ denote the minimum number of bond-edge types needed to construct G . Thus, the goal is to find $T_i(G)$ and $B_i(G)$ for graphs that represent DNA complexes.

1.4 Goal for the Project

Since the study of DNA self-assembly is relatively new, there are plenty of open questions that are waiting to be asked. The article [EMPB⁺14] has results for the DNA self-assembly of some standard classes of graphs. The classes of graphs that will be particularly interesting will be k -regular graphs and complete graphs since the rook's graph is both regular and the Cartesian product of complete graphs. In Scenario 1 we will use the theory developed for regular graphs and in Scenario 2, we will use the theory developed for complete graphs to build a pot for the rook's graph. Using the fact that the rook's graph is regular, $T_1(G)$ and $B_1(G)$ follow easily from [EMPB⁺14]. We will devote Chapter 3 to describing the pots of tiles that realize a rook's graph in Scenario 1. Since there has already been theory developed for a complete graph K_n in [EMPB⁺14], we attempt to build the rook's graph relying on the structure of the tiles and bond-edge types for complete graphs. In Chapter 2, we take a deeper look at the theory needed for the DNA self assembly of the rook's graph. Then we will look at Scenario 1 and Scenario 2 in Chapters 3 and 4.

Chapter 2

Necessary Information About DNA Self-Assembly

2.1 Background Information

Most of the theory and the results in this chapter are found in [EMPB⁺14]. One proposition that will provide bounds for $T_i(G)$ and $B_i(G)$ is the following:

Proposition 2.1. *For any graph G , $B_1(G) \leq B_2(G) \leq B_3(G)$ and $T_1(G) \leq T_2(G) \leq T_3(G)$.*

This proposition will help provide bounds in later chapters. The next definition gives notation that will appear shortly.

Definition 2.2. *Given a pot P , define $\mathcal{O}(P)$ to be the set of graphs realized by P . The set of graphs of minimum order that may be realized by P is denoted $\mathcal{O}_{\min}(P)$. Denote m_p for the minimal order of a graph that may be realized by P .*

Furthermore, given a pot $P = \{t_1, \dots, t_p\}$, define $A_{i,j}$ to be the number of cohesive-ends of type a_i on tile t_j , and $\hat{A}_{i,j}$ to be the number of cohesive-ends of type \hat{a}_i . With the preceding definition, the following proposition follows from requiring the complexes to be complete.

Proposition 2.3. *Let $P = \{t_1, \dots, t_p\}$ be a pot. Then :*

1. *The total number of hatted cohesive-ends types must equal the total number of unhatted cohesive-end types in a complete complex.*
2. *If $G \in \mathcal{O}(P)$ where the order of G is n , then there are nonnegative integers R_j for $j = 1, \dots, p$ (representing the number of each tile of the type t_j used in the construction of G) with $\sum_j R_j = n$ and such that $\sum_j R_j(A_{i,j} - \hat{A}_{i,j}) = 0$ for all i . That is, the number of hatted cohesive-ends of each type used in the construction of G must equal the number of unhatted cohesive-ends of the same type that appear in the construction.*

This information is then encoded in a matrix with the following definition. Also, the following definition and proposition along with Proposition 2.3 will be used extensively to prove results in later chapters while working in Scenario 1 and Scenario 2.

Definition 2.4. *Let P be a pot with p tile types labeled t_1, \dots, t_p and let $z_{i,j}$ be the net number of cohesive-ends of type a_i on tile t_j , i.e., $z_{i,j} = A_{i,j} - \hat{A}_{i,j}$. Define r_i to be the proportion of tile type t_i used in the assembly process. The following system of equations captures the requirements outlined in Item 2 of Proposition 2.3:*

$$\begin{aligned} z_{1,1}r_1 + z_{1,2}r_2 + \dots + z_{1,p}r_p &= 0 \\ &\vdots \\ z_{m,1}r_1 + z_{m,2}r_2 + \dots + z_{m,p}r_p &= 0 \\ r_1 + r_2 + \dots + r_p &= 1 \end{aligned}$$

The construction matrix of P , $M(P)$, is the corresponding augmented matrix:

$$M(P) = \left[\begin{array}{cccc|c} z_{1,1} & z_{1,2} & \dots & z_{1,p} & 0 \\ \vdots & \vdots & & \vdots & \\ z_{m,1} & z_{m,2} & \dots & z_{m,p} & 0 \\ 1 & 1 & \dots & 1 & 1 \end{array} \right] \quad (2.1)$$

The solution space of the construction matrix $M(P)$ of a pot P is called the spectrum of P and is denoted $\mathcal{S}(P)$.

Proposition 2.5. *Let $P = \{t_1, \dots, t_p\}$ be a pot. Then:*

1. *If G is a graph of order n where $G \in \mathcal{O}(P)$ using R_j tiles of type t_j , then $(1/n)\langle R_1, \dots, R_p \rangle \in \mathcal{S}(P)$.*
2. *If $\langle r_1, \dots, r_p \rangle \in \mathcal{S}(P)$, and there is a positive integer n such that $nr_j \in \mathbb{Z}_{\geq 0}$ for all j , then there is a graph of order n such that $G \in \mathcal{O}(P)$ using nr_j tiles of type t_j .*
3. *The minimum order of a graph realized by P is $m_p = \min\{\text{lcm}\{b_j \mid r_j \neq 0 \text{ and } r_j = a_j/b_j\}, \text{ where } \langle r_1, \dots, r_p \rangle \in \mathcal{S}(P)\}$, and where the minimum is taken over all solutions to $M(P)$ such that $r_j \geq 0$ and a_j/b_j is in reduced form for all j .*

2.2 Information for Scenario 1

We develop a few tools for Scenario 1 before exploring the results for the rook's graph in Chapter 3. The *valency sequence* of G is the sequence of unique vertex degrees of G , and the length of the sequence is denoted $av(G)$. The *even-valency sequence* is the sequence of unique even degree vertices of G , with its length denoted $ev(G)$. Lastly, the *odd-valency sequence* is the sequence of unique odd degree vertices of G , with its length denoted $ov(G)$. According to [EMPB⁺14] the algorithm that appears here as Algorithm 2.7 produces a pot where $av(G) \leq T_1(G) \leq ev(G) + 2ov(G)$, and $B_1(G) = 1$. Recall that an *Eulerian graph* is a connected graph that contains an Eulerian circuit [CZ12]. A useful theorem in [CZ12] states that a nontrivial connected graph G is Eulerian if and only if every vertex of G has even degree. An algorithm that will be used within Algorithm 2.7 along with results in later chapters is called *Fleury's Algorithm*. Fleury's Algorithm is used to display the Euler path or Euler circuit from a given graph.

Algorithm 2.6 (Fleury's Algorithm). *In this algorithm one labels the edges in the order in which they are traveled.*

1. *Make sure the graph is connected and has no odd degree vertices.*
2. *Make two copies of the graph, and label them G_1 and G_2 .*
3. *Choose a starting vertex.*

4. At each step, label the edge being traversed in G_1 by giving it an orientation and delete the corresponding edge in G_2 . If there is a choice between a bridge and a non-bridge, always choose the non-bridge to traverse.
5. Once every edge in G_1 is traversed, the circuit is complete and you should be back at the starting vertex.

Algorithm 2.7. Input: a target graph G .

Output: at most $ev(G) + 2ov(G)$ tile types from which G may be constructed.

1. Create an augmented graph G' from G by adding edges between pairs of odd degree vertices. G' is then Eulerian.
2. Use Fleury's Algorithm to find a directed Eulerian circuit.
3. Delete the augmented edges, leaving an orientation \vec{G} of the original graph G .
4. Record a tile type with j cohesive-ends of type a and k cohesive-ends of type \hat{a} whenever there is a vertex of \vec{G} with outdegree j and indegree k .

This algorithm ensures that $B_1(G) = 1$ for all graphs and ensures that at most $ev(G) + 2ov(G)$ tile types are used. A consequence of the algorithm is the following corollary as presented in [EMPB⁺14]:

Corollary 2.8. *If G is a k -regular graph, then*

$$T_1(G) = \begin{cases} 1 & \text{if } k \text{ is even,} \\ 2 & \text{if } k \text{ is odd.} \end{cases}$$

We shall use the terminology of *even regular* if G is k -regular where k is even and *odd regular* if k is odd.

2.3 Information for Scenario 2

For Scenario 2, we explore pots that realize structures no smaller than the order of the desired graph. There are two results from [EMPB⁺14], that will be used in Chapter 4. The first theorem gives a relationship between the number of bond-edge types and the number of tile types needed to realize a structure.

Theorem 2.9. *If G is a graph with $n > 2$ vertices, then $B_2(G) + 1 \leq T_2(G)$.*

The next result gives the minimum number of bond-edge types and tile types for the complete graph, K_n .

Proposition 2.10.

$$B_2(K_n) = \begin{cases} 1 & \text{if } n \text{ is even,} \\ 2 & \text{if } n \text{ is odd.} \end{cases}$$

$$T_2(K_n) = \begin{cases} 2 & \text{if } n \text{ is even,} \\ 3 & \text{if } n \text{ is odd.} \end{cases}$$

A helpful portion in the proof of the previous proposition is the description of the tiles used to realize K_n . The pots are

$$P_{\text{even}} = \{t_1 = \{a^{n-1}\}, t_2 = \{\hat{a}^{n/2}, a^{n/2-1}\}\} \quad (2.2)$$

$$P_{\text{odd}} = \{t_1 = \{a^{n-1}\}, t_2 = \{\hat{a}, b^{(n-3)/2}, \hat{b}^{(n-1)/2}\}, t_3 = \{\hat{a}, b^{(n-1)/2}, \hat{b}^{(n-3)/2}\}\}. \quad (2.3)$$

Chapter 3

Rooks Graph Under Scenario 1

3.1 Method Used for the Construction

In constructing the self-assembly design of the rook's graph, the ideas discussed in Chapter 2, Section 2 will be implemented. We will also consider the graph theory developed in Section 1.1.2 with a little more detail. First, we will use Corollary 2.8 to determine the number of tile types needed to build the rook's graph. Then an explicit description of the pot of tiles used in its construction is given. The results from [EMPB⁺14] were used in conjunction with Fleury's algorithm to discover the explicit form of the tiles. Notice in the case when $m = 1$ the $m \times n$ rook's graph is K_n . Also, note the 2×2 rook's graph is C_4 , the cycle graph on 4 vertices. Thus, for the rest of this chapter, we assume $m \geq 2$ and $n > 2$.

3.2 $n \times n$ Rook's Graph

Lemma 3.1. *The $n \times n$ rook's graph is even regular.*

Proof. Consider an $n \times n$ grid and choose any arbitrary point of the grid. A rook's piece can move to any other point in that column. That is, there are $n - 1$ moves in that column. Utilizing the same line of reasoning, a rook's piece can also move to any other point on that row, that is, there are $n - 1$ moves in that row. Hence each vertex has degree $(n - 1) + (n - 1) = 2(n - 1)$. Hence G is even regular. \square

By Theorem 3.3 $P = \{t_1 = \{a^2, \hat{a}^2\}\}$. Note that P realizes regular graphs of any order as long as the degree of each vertex is 4.

3.3 $m \times n$ Rook's Graph

In the case where $m \neq n$, we assume $m < n$ since an $m \times n$ rook's graph with $m > n$ will be isomorphic. That is, a 2×7 rook's graph is isomorphic to the 7×2 rook's graph.

Lemma 3.5. *Let G be an $m \times n$ rook's graph where $m < n$. If m and n are of the same parity then G is even regular. If m and n are not of the same parity, then G is odd regular.*

Proof. Consider an $m \times n$ grid where $m < n$. There are three cases depending on the parity of m and n . Note that each vertex has degree $(m - 1) + (n - 1) = m + n - 2$.

Case one, assume m and n are both even. Then $m = 2k$ and $n = 2q$ where $k, q \in \mathbb{N}$. Then each vertex has degree $m + n - 2 = 2k + 2q - 2 = 2(k + q - 1)$. That is every vertex is of even degree, and G is even regular.

Case two, assume m and n are both odd. Then $m = 2a + 1$ and $n = 2b + 1$ where $a, b \in \mathbb{N}$. Then each vertex has degree $m + n - 2 = (2a + 1) + (2b + 1) - 2 = 2a + 2b = 2(a + b)$. Hence every vertex is of even degree and G is even regular.

Case three, without loss of generality assume m is even and n is odd. Thus $m = 2c$ and $n = 2d + 1$ where $c, d \in \mathbb{N}$. Then each vertex has degree $m + n - 2 = (2c) + (2d + 1) - 2 = 2c + 2d - 2 + 1 = 2(c + d - 1) + 1$. Hence each vertex is of odd degree and G is odd regular.

Hence if m and n are of the same parity, then G is even regular. If m and n are not of the same parity, then G is odd regular. \square

Lemma 3.6. *Let G be an $m \times n$ rook's graph where $m < n$. If m and n are of the same parity then $T_1(G) = 1$ and $B_1(G) = 1$.*

Proof. Let G be an $m \times n$ rook's graph where $m < n$. By Corollary 2.8, $T_1(G) = 1$. By Algorithm 2.7, $B_1(G) = 1$. \square

Theorem 3.7. *Let G be an $m \times n$ rook's graph, where $m < n$. If m and n are of the same parity and $P = \left\{ t = \left\{ a^{\frac{(m-1)+(n-1)}{2}}, \hat{a}^{\frac{(m-1)+(n-1)}{2}} \right\} \right\}$, then $G \in \mathcal{O}(P)$.*

Proof. Given an $m \times n$ rook's graph G , where $m < n$ and m and n are of the same parity, by Lemma 3.5 every degree is even and $\deg(v) = (m - 1) + (n - 1)$ for all $v \in V$. By Lemma

3.6, $T_1(G) = 1$ and $B_1(G) = 1$. Hence $P = \{t\}$ where $t = \{a^k, \hat{a}^{(m-1)+(n-1)-k}\}$ for some $k \in \{0, 1, 2, \dots, (m-1)+(n-1)\}$. According to Proposition 2.3 part 2, $R_1(A_{1,1} - \hat{A}_{1,1}) = 0$, where $R_1 = mn$ which implies that $A_{1,1} = \hat{A}_{1,1}$. Thus $k = (m-1) + (n-1) - k$ which yields that $k = \frac{(m-1)+(n-1)}{2}$. As a consequence of using Algorithm 2.7, $G \in \mathcal{O}(P)$. \square

Example 3.8. Consider the 2×4 rook's graph. Note that $\deg(v) = 4$ for all $v \in V$. Implementing Fleury's Algorithm, the following picture is constructed.

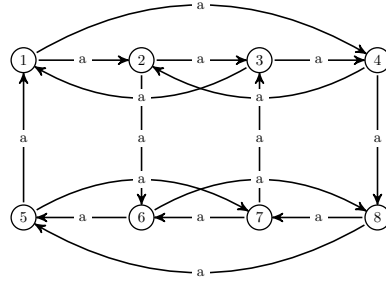


Figure 3.2: 2×4 rook's graph in Scenario 1

By Theorem 3.7, $P = \{t_1 = \{a^2, \hat{a}^2\}\}$. Note that P realizes regular graphs of any order as long as the degree of each vertex is 4. Note that the pot P in this example is the same pot as in Example 3.4. This is permitted in Scenario 1.

Theorem 3.9. Let G be an $m \times n$ rook's graph, where $m < n$. If m and n are not of the same parity and $P = \left\{t_1 = \left\{a^{\frac{m+n-1}{2}}, \hat{a}^{\frac{m+n-3}{2}}\right\}, t_2 = \left\{a^{\frac{m+n-3}{2}}, \hat{a}^{\frac{m+n-1}{2}}\right\}\right\}$, then $G \in \mathcal{O}(P)$.

Proof. Given an $m \times n$ rook's graph G , where $m < n$ and m and n are not of the same parity, by Lemma 3.5 every degree is odd. By Corollary 2.8, $T_1(G) = 2$ and by Algorithm 2.7, $B_1(G) = 1$. By Lemma 3.5 $\deg(v) = (m-1) + (n-1) = m+n-2$ for all $v \in V$. Since Algorithm 2.7 augments the graph and builds an Eulerian circuit, once deleting the augmented edges, the number of incoming and outgoing edges in each vertex differs by one. That is, the number of cohesive-ends a and \hat{a} differs by one in each tile. To achieve this, the tiles will have the form $t_1 = \{a^k, \hat{a}^{k-1}\}$ and $t_2 = \{a^l, \hat{a}^{l+1}\}$. Then $k + (k-1) = m+n-2$ implies $k = \frac{m+n-1}{2}$. Similarly, $l + (l+1) = m+n-2$ implies $l = \frac{m+n-3}{2}$. As a consequence of using Algorithm 2.7, $G \in \mathcal{O}(P)$. \square

Chapter 4

Rook's Graph Under Scenario 2

The idea behind the construction of the rook's graph under Scenario 2 was to use the theory already developed for $T_2(K_n)$ and $B_2(K_n)$ from [EMPB⁺14]. This idea worked for the $2 \times n$ rook's graph where n is odd. A different method of constructing the remaining classes of rook's graphs had to be developed, which yielded the pot for the general $n \times n$ case. As in Chapter 3, in the case when $m = 1$ the $m \times n$ rook's graph is K_n . Also, note the 2×2 rook's graph is C_4 , the cycle graph on 4 vertices. Thus, for the rest of this chapter, we assume $m \geq 2$ and $n > 2$ with the exception of Theorem 4.7 and Theorem 4.12.

4.1 $2 \times n$ Rook's Graph.

Theorem 4.1. *If G is a $2 \times n$ rook's graph, then $B_2(G) \geq 2$.*

Proof. Assume by contradiction that $B_2(G) = 1$. The associated construction matrix for pots with one bond-edge type has the form

$$M(P) = \left[\begin{array}{cccc|c} z_{1,1} & z_{1,2} & \dots & z_{1,p} & 0 \\ 1 & 1 & \dots & 1 & 1 \end{array} \right],$$

which has a solution of the form

$$\frac{1}{(z_{1,1} - z_{1,2})} \langle -z_{1,2}, z_{1,1}, 0, \dots, 0 \rangle \in \mathcal{S}(P). \quad (4.1)$$

Note that $z_{1,j} \neq 0$ for all j otherwise a graph of order 1 may be realized. Reorder the tiles as necessary so that $z_{1,1} > 0$ and $z_{1,2} < 0$. Since $\deg(v) = n$ for all $v \in V$, then $|z_{1,j}| \leq n$. This implies that $z_{1,1} - z_{1,2} \leq 2n$. If $z_{1,1} - z_{1,2} = 2n$, this implies $t_1 = \{a^n\}$ and $t_2 = \{\hat{a}^n\}$. Then the solution from Equation 4.1 is of the form $\langle \frac{n}{2n}, \frac{n}{2n}, 0, \dots, 0 \rangle$ which can be rewritten as $\langle \frac{1}{2}, \frac{1}{2}, 0, \dots, 0 \rangle$. This implies that a graph of order 2 may be realized which is less than the order of G . If $z_{1,1} - z_{1,2} < 2n$, then P realizes a graph of order smaller than the target graph of order $2n$, a contradiction. Thus $B_2(G) \geq 2$. \square

Corollary 4.2. *If G is a $2 \times n$ rook's graph, then $T_2(G) \geq 3$.*

Proof. Since G is a $2 \times n$ rook's graph, we have by Theorem 4.1 that $B_2(G) \geq 2$. By Theorem 2.9 we have that $T_2(G) \geq 3$. \square

Notice that Theorem 4.1 tells us the pots that realize a rook's graph in Scenario 1 will not satisfy the conditions of Scenario 2. Therefore, we need a new design strategy.

First method of constructing pots.

The goal for finding an assembly design of the $2 \times n$ rook's graph when n is odd is to take the complete graph K_n along with its tile structure from Equation 2.3 and “flatten it out”. That is, rearrange the vertices such that they make a straight line using the tiles $t_1 = \{a^{n-1}\}$, $t_2 = \{\hat{a}, b^{(n-3)/2}, \hat{b}^{(n-1)/2}\}$, $t_3 = \{\hat{a}, b^{(n-1)/2}, \hat{b}^{(n-3)/2}\}$ to represent the vertices. More formally, let

$$\lambda(v_i) = \begin{cases} t_1, & \text{for } i \in \{1, 2n\} \\ t_2, & \text{for } i \in \{2, \dots, \frac{n+1}{2}\} \cup \{\frac{3n+1}{2}, \dots, 2n-1\} \\ t_3, & \text{for } i \in \{\frac{n+3}{2}, \dots, \frac{3n-1}{2}\}. \end{cases} \quad (4.2)$$

For example, the 2×5 rook's graph yields the following assembly design as in Figure 4.1b, and Figure 4.1c

$$\lambda(v_i) = \begin{cases} t_1, & \text{for } i \in \{1, 10\} \\ t_2, & \text{for } i \in \{2, 3, 8, 9\} \\ t_3, & \text{for } i \in \{4, 5, 6, 7\}. \end{cases}$$

Next, “stack” the K_n copies as in Figure 4.2a and “glue” the graphs together to construct the entire $2 \times n$ rook's graph. By the design of K_n , vertices v_i for $i \in$

$\{2, \dots, \frac{n+1}{2}\} \cup \{\frac{3n+1}{2}, \dots, 2n-1\}$ have one more cohesive-end \hat{b} than cohesive-end b and vertices v_k for $k \in \{\frac{n+3}{2}, \dots, \frac{3n-1}{2}\}$ have one more cohesive-end b than cohesive-end \hat{b} . To “glue” K_2 and K_n , let v_i for $i \in \{1, \dots, \frac{n-1}{2}\} \cup \{\frac{3n+1}{2}, \dots, 2n\}$ receive the cohesive-end b and let vertices v_k for $k \in \{\frac{n+1}{2}, \dots, \frac{3n-1}{2}\}$ receive the cohesive-end \hat{b} .

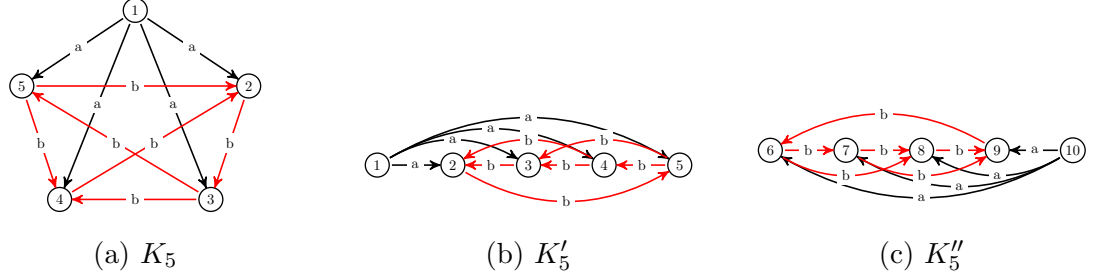


Figure 4.1: Complete graph K_5 and an isomorphic copy

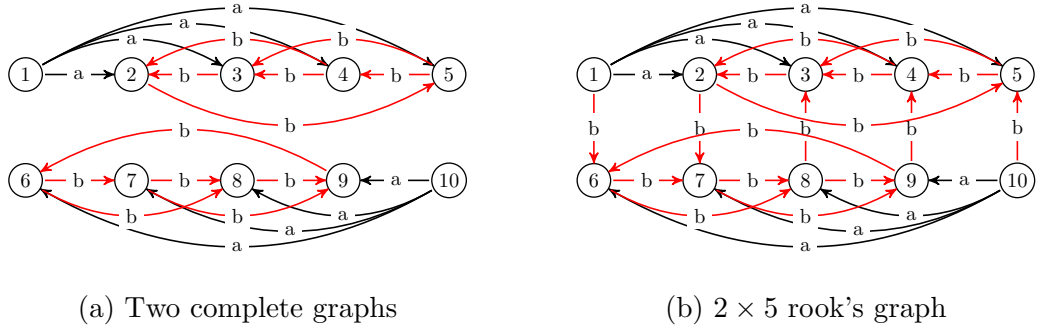


Figure 4.2: Making a rook's graph from two complete graphs

Note that this construction only works for the $2 \times n$ rook's graph where n is odd. This method does not work for the $2 \times n$ case where n is even due to the fact that a graph of smaller order is always realized. This was discovered by looking at the spectrum. According to Theorem 4.1, $B_2(G) \geq 2$ and by Theorem 2.9, $T_2(G) \geq 3$. Since $B_2(G) \geq 2$, we have that in the “stacking” and “gluing” process using $P_{\text{even}} = \{t_1 = \{a^{n-1}\}, t_2 = \{\hat{a}^{n/2}, a^{n/2-1}\}\}$ from Equation 2.2, we are forced to use a new bond-edge type b . This yields $P = \{t_1 = \{a^{n-1}, b\}, t_2 = \{\hat{a}^{n/2}, a^{n/2-1}, b\}, t_3 = \{\hat{a}^{n/2}, a^{n/2-1}, \hat{b}\}\}$. Thus, the construction matrix $M(P)$ has the unique solution $\langle \frac{1}{n}, \frac{n-2}{2n}, \frac{1}{2} \rangle$. Since n is even, the ratio $\frac{n-2}{2n}$ can be reduced and we have that $m_p = n$. Thus there exists a graph $H \in \mathcal{O}(P)$ such that the order of H is n .

The following is an example of the 2×3 rook's graph following the first method of constructing pots.

Example 4.3. Consider the 2×3 rook's graph. Let the colors black and red represent the bond-edge types a , b , respectively.

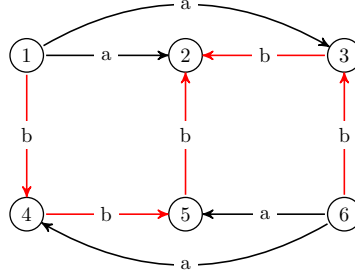


Figure 4.3: 2×3 rook's graph

Consider the following tiles: $t_1 = \{a^2, b\}$, $t_2 = \{\hat{a}, b, \hat{b}\}$, $t_3 = \{\hat{a}, \hat{b}^2\}$. Hence the pot $P = \{t_1, t_2, t_3\}$, has the associated construction matrix

$$M(P) = \left[\begin{array}{ccc|c} 2 & -1 & -1 & 0 \\ 1 & 0 & -2 & 0 \\ 1 & 1 & 1 & 1 \end{array} \right]$$

with solution $\langle \frac{1}{3}, \frac{1}{2}, \frac{1}{6} \rangle \in \mathcal{S}(P)$ and $m_p = 6$.

This example and method of constructing pots leads to the following proposition.

Proposition 4.4. If G is a $2 \times n$ rook's graph where n is odd, then $B_2(G) = 2$ and $T_2(G) = 3$.

Proof. Let $P = \{t_1 = \{a^{n-1}, b\}, t_2 = \{\hat{a}, b^{\frac{n-1}{2}}, \hat{b}^{\frac{n-1}{2}}\}, t_3 = \{\hat{a}, b^{\frac{n-3}{2}}, \hat{b}^{\frac{n+1}{2}}\}\}$. This yields the following construction matrix

$$M(P) = \left[\begin{array}{ccc|c} n-1 & -1 & -1 & 0 \\ 1 & 0 & -2 & 0 \\ 1 & 1 & 1 & 1 \end{array} \right]$$

which has solution $\langle \frac{1}{n}, \frac{2n-3}{2n}, \frac{1}{2n} \rangle \in \mathcal{S}(P)$ and applying Proposition 2.5 item 3, $m_p = 2n$. Thus $B_2(G) = 2$ and according to Corollary 4.2, $T_2(G) \geq 3$. By construction $\#P = 3$, hence $T_2(G) = 3$. Note $G \in \mathcal{O}_{min}(P)$ by the construction of P . \square

Second method of constructing pots.

To discover a pot that will realize the $2 \times n$ rook's graph where n is even, the idea was to think “backwards” and reverse engineer what is wanted. We assume that $B_2(G) = 2$, and that $T_2(G) = 3$. By Theorem 4.1 and Corollary 4.2 we know $B_2(G) \geq 2$ and $T_2(G) \geq 3$, so these assumptions are reasonable. Then there is a solution of the form $\frac{1}{2n}\langle R_1, R_2, R_3 \rangle \in \mathcal{S}(P)$. According to Proposition 2.3 Item 2, the following system of equations are produced:

$$z_{1,1}R_1 + z_{1,2}R_2 + z_{1,3}R_3 = 0 \quad (4.3)$$

$$z_{2,1}R_1 + z_{2,2}R_2 + z_{2,3}R_3 = 0 \quad (4.4)$$

$$R_1 + R_2 + R_3 = 2n. \quad (4.5)$$

We use the 2×4 rook's graph as an example to motivate the construction. For this example, there are two more assumptions that were made. Assume $R_1 = 2$ and $t_1 = \{a^3, b\}$, then $\langle \frac{2}{8}, \frac{R_2}{8}, \frac{R_3}{8} \rangle \in \mathcal{S}(P)$. Since the order of the target graph is 8, and two vertices have already been identified to a tile, this results in $R_2 + R_3 = 6$. The choice of R_2 and R_3 is then refined due to the fact that one can not choose both R_2 and R_3 to be even. Let $R_2 = 5$ and $R_3 = 1$, then Equation 4.3 and Equation 4.4 become

$$3(2) + z_{1,2}(5) + z_{1,3}(1) = 0 \quad (4.6)$$

$$1(2) + z_{2,2}(5) + z_{2,3}(1) = 0 \quad (4.7)$$

which yields

$$M(P) = \left[\begin{array}{ccc|c} 3 & z_{1,2} & z_{1,3} & 0 \\ 1 & z_{2,2} & z_{2,3} & 0 \\ 1 & 1 & 1 & 1 \end{array} \right].$$

By letting $z_{i,2}$ be the x -axis and letting $z_{i,3}$ be the y -axis we obtain the following graph. Keep in mind that $|z_{i,j}| \leq \deg(v) = 4$ which bounds the graph as in Figure 4.4. We look for lattice points on the lines in Equations 4.6 and 4.7. Once all possible lattice points are found, we sift through the corresponding tiles to see if they build the desired graph.

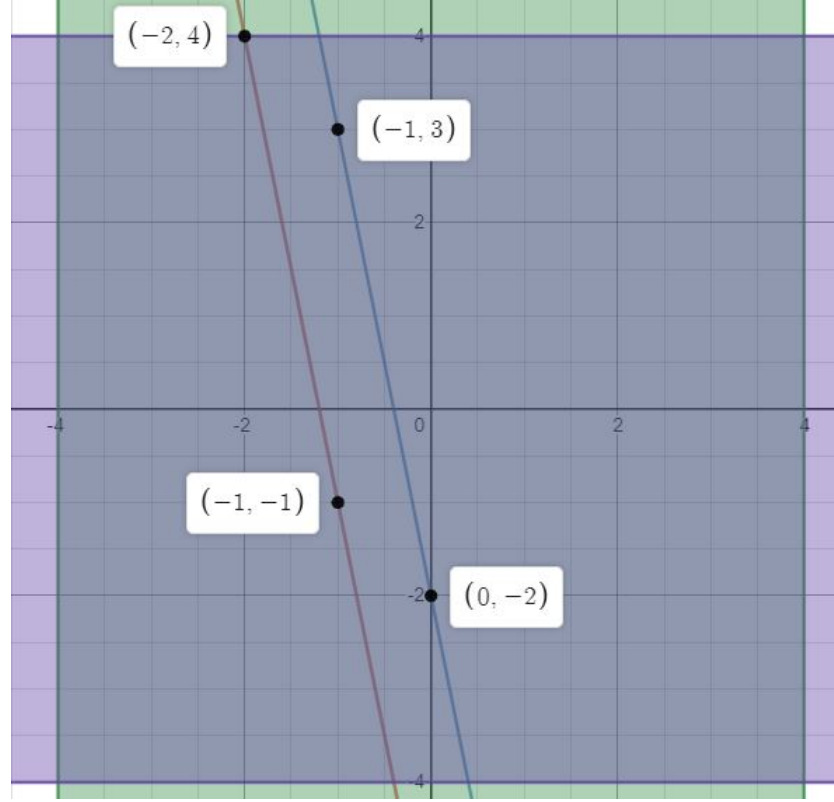


Figure 4.4: Lattice points

Continuing our motivation with the 2×4 example, $(z_{1,2}, z_{1,3}) \in \{(-2, 4), (-1, -1)\}$ and $(z_{2,2}, z_{2,3}) \in \{(-1, 3), (0, -2)\}$. If $(z_{1,2}, z_{1,3}) = (-2, 4)$, then $z_{1,3} = 4$ implies t_3 has at least 4 cohesive-ends of type a . Since $\deg(v) = 4$ for all $v \in V$, t_3 has no cohesive-ends of type \hat{a}, b or \hat{b} . Hence $z_{2,3} = 0$, a contradiction. This leaves us with $(z_{1,2}, z_{1,3}) = (-1, -1)$. If $z_{i,j}$ is odd, then the sum of cohesive-ends from a particular bond-edge type must be odd. That is, $z_{1,2} = -1$ implies t_2 has the cohesive-ends $\{\hat{a}\}$ or $\{a, \hat{a}^2\}$. If $z_{i,j}$ is even, then the sum of cohesive-ends from a particular bond-edge type must be even. That is, $z_{2,2} = 0$ implies t_2 has cohesive-ends $\{b, \hat{b}\}$ or $\{b^2, \hat{b}^2\}$. Since $\deg(v) = 4$ for all $v \in V$, we must have 4 cohesive-ends per tile. Hence if $(z_{1,2}, z_{1,3}) = (-1, -1)$, then $(z_{2,2}, z_{2,3}) \neq (0, -2)$. Therefore, $(z_{1,2}, z_{1,3}) = (-1, -1)$ and $(z_{2,2}, z_{2,3}) = (-1, 3)$. This means $t_2 = \{\hat{a}, b, \hat{b}^2\}$ or $t_2 = \{a, \hat{a}^2, \hat{b}\}$, and $t_3 = \{\hat{a}, b^3\}$. After attempting to build our graph, the pot found in Example 4.5 is the only set of tiles that constructs the 2×4 rook's graph under our assumptions.

Example 4.5. Consider the 2×4 rook's graph and the following tiles: $t_1 = \{a^3, b\}$, $t_2 = \{\hat{a}, b, \hat{b}^2\}$, $t_3 = \{\hat{a}, b^3\}$. Hence the pot $P = \{t_1, t_2, t_3\}$, has the associated construction matrix

$$M(P) = \left[\begin{array}{ccc|c} 3 & -1 & -1 & 0 \\ 1 & -1 & 3 & 0 \\ 1 & 1 & 1 & 1 \end{array} \right]$$

with solution $\langle \frac{1}{4}, \frac{5}{8}, \frac{1}{8} \rangle \in \mathcal{S}(P)$ and $m_P = 8$. Let the colors black and red represent the bond-edge types a , b , respectively.

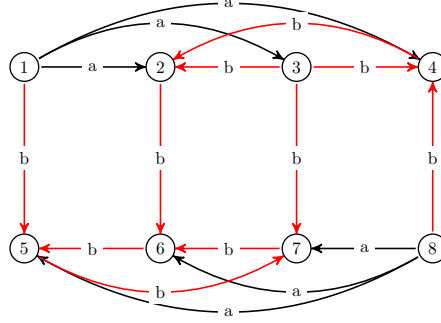


Figure 4.5: 2×4 rook's graph

This example leads to the following conjecture.

Conjecture 4.6. If G is a $2 \times n$ rook's graph where $n = 4k$ and $k \in \mathbb{N}$, then $B_2(G) = 2$ and $T_2(G) = 3$.

Let $P = \{t_1 = \{a^{n-1}, b\}, t_2 = \{\hat{a}, b^{(n-2)/2}, \hat{b}^{n/2}\}, t_3 = \{\hat{a}, b^{(n/2)+1}, \hat{b}^{(n/2)-2}\}\}$.

The associated construction matrix is

$$M(P) = \left[\begin{array}{ccc|c} n-1 & -1 & -1 & 0 \\ 1 & -1 & 3 & 0 \\ 1 & 1 & 1 & 1 \end{array} \right]$$

with solution

$$\left\langle \frac{1}{n}, \frac{3n-2}{4n}, \frac{n-2}{4n} \right\rangle \in \mathcal{S}(P). \quad (4.8)$$

Since $n = 4k$ where $k \in \mathbb{N}$, the solution in Equation 4.8 becomes

$$\left\langle \frac{1}{4k}, \frac{6k-1}{8k}, \frac{2k-1}{8k} \right\rangle. \quad (4.9)$$

By Proposition 2.5 item 3, $m_p = 8k = 2n$.

It still remains to be shown that $G \in \mathcal{O}_{\min}(P)$ for all $2 \times n$ rook's graphs where $n = 4k$ for $k \in \mathbb{N}$. That is, it needs to be shown that there exists an explicit assembly design using the pot P in Conjecture 4.6. Example 4.5 shows that P realizes the 2×4 rook's graph and it has been shown that P also realizes the 2×8 and the 2×12 rook's graph with the following assembly design

$$\lambda(v_i) = \begin{cases} t_1, & \text{for } i \in \{1, 2n\} \\ t_2, & \text{for } i \notin \{1, 3, 5, \dots, n-1, 2n\} \\ t_3, & \text{for } i \in \{3, 5, 7, \dots, n-1\}. \end{cases} \quad (4.10)$$

We leave it as a conjecture that $G \in \mathcal{O}_{\min}(P)$ for all $n = 4k$. When $n = 4k + 2$ for some $k \in \mathbb{N}$, the pot in Conjecture 4.6 realizes a graph of order n . That is, the unique solution $\langle \frac{1}{n}, \frac{3n-2}{4n}, \frac{n-2}{4n} \rangle$ from Equation 4.8 can be rewritten as $\langle \frac{1}{4k+2}, \frac{3k+1}{4k+2}, \frac{k}{4k+2} \rangle$, hence $m_p = 4k + 2 = n$.

4.2 $m \times n$ Rook's Graph

We build upon the results of Section 4.1 to prove in general, $B_2(G) \geq 2$.

Theorem 4.7. *If G is an $m \times n$ rook's graph where $m > 2$ and $n > 2$ and $m \leq n$, then $B_2(G) \geq 2$.*

Proof. Assume by contradiction that $B_2(G) = 1$. The associated construction matrix for pots with one bond-edge type has the form

$$M(P) = \left[\begin{array}{ccccc|c} z_{1,1} & z_{1,2} & z_{1,3} & \cdots & z_{1,p} & 0 \\ 1 & 1 & 1 & \cdots & 1 & 1 \end{array} \right],$$

which has a solution of the form

$$\frac{1}{(z_{1,1} - z_{1,2})} \langle -z_{1,2}, z_{1,1}, 0, \dots, 0 \rangle \in \mathcal{S}(P).$$

Note that $z_{1,j} \neq 0$ for all j otherwise a graph of order 1 may be realized. Reorder the tile numbers as necessary so that $z_{1,1} > 0$ and $z_{1,2} < 0$. Furthermore, since $\deg(v) = (m-1) + (n-1)$ for all $v \in V$, then $|z_{i,j}| \leq (m-1) + (n-1)$. This implies that $z_{1,1} - z_{1,2} \leq 2[(m-1) + (n-1)] = 2[m+n-2]$. Note that $0 < (m-2)(n-2)$ for $m > 2$ and $n > 2$, thus $z_{1,1} - z_{1,2} \leq 2[m+n-2] < mn$. This would imply P realizes a graph of order less than G , a contradiction, hence $B_2(G) \geq 2$. \square

Corollary 4.8. *If G is an $m \times n$ rook's graph where $m > 2$ and $n > 2$, then $T_2(G) \geq 3$.*

Proof. Since G is an $m \times n$ rook's graph where $m > 2$ and $n > 2$ we have by Theorem 4.7 that $B_2(G) \geq 2$. By Theorem 2.9 we have that $T_2(G) \geq 3$. \square

The following example shows that for the 3×4 rook's graph, $B_2(G) = 2$ and $T_2(G) = 3$.

Example 4.9. *Consider the 3×4 rook's graph. Let the colors black and red represent the bond-edge types a , b , respectively.*

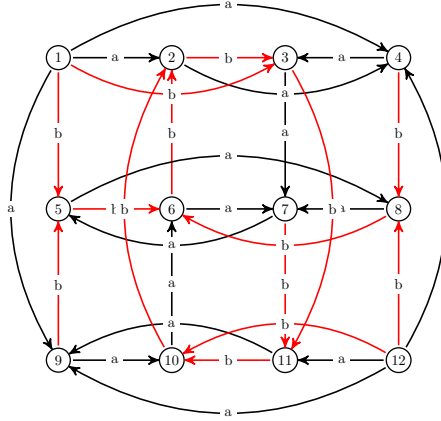


Figure 4.6: 3×4 rook's graph

Consider the following tiles: $t_1 = \{a^3, b^2\}$, $t_2 = \{a, \hat{a}, b, \hat{b}^2\}$, $t_3 = \{a, \hat{a}^3, b\}$. Hence the pot $P = \{t_1, t_2, t_3\}$, has the associated construction matrix

$$M(P) = \left[\begin{array}{ccc|c} 3 & 0 & -2 & 0 \\ 2 & -1 & 1 & 0 \\ 1 & 1 & 1 & 1 \end{array} \right]$$

with solution $\langle \frac{1}{6}, \frac{7}{12}, \frac{1}{4} \rangle \in \mathcal{S}(P)$ and $m_p = 12$.

4.3 $n \times n$ Rook's Graph

The next two examples show the design process for the $n \times n$ rook's graph. Using the second method of constructing pots, as in the $2 \times n$ case, we begin by making a set of reasonable assumptions. We assume $R_1 = 1$ and $t_1 = \{a^{2(n-1)}\}$. We then generalize these examples in Theorem 4.12.

Example 4.10. Consider the 3×3 rook's graph. Let the colors black and red represent the bond-edge types a , b , respectively. The graph is built in two phases as in Figure 4.7. To complete the construction, superimpose Figure 4.7a and Figure 4.7b.

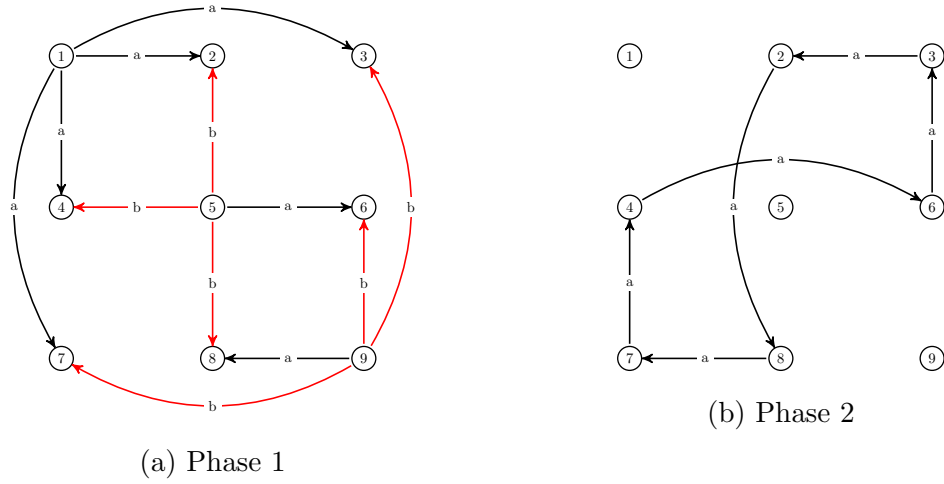


Figure 4.7: 3×3 rook's graph

Consider the following tiles: $t_1 = \{a^4\}$, $t_2 = \{a, \hat{a}^2, \hat{b}\}$, $t_3 = \{a, b^3\}$. Hence the pot $P = \{t_1, t_2, t_3\}$, has the associated construction matrix

$$M(P) = \left[\begin{array}{ccc|c} 4 & -1 & 1 & 0 \\ 0 & -1 & 3 & 0 \\ 1 & 1 & 1 & 1 \end{array} \right]$$

with solution $\langle \frac{1}{9}, \frac{2}{3}, \frac{2}{9} \rangle \in \mathcal{S}(P)$ and $m_P = 9$.

In Phase 1 of Figure 4.7a, let

$$\lambda(v_i) = \begin{cases} t_1 & \text{for } i \in \{1\} \\ t_3 & \text{for } i \in \{5, 9\}. \end{cases}$$

Note that t_1 only has one choice for distributing its cohesive-ends. For tile t_3 distribute the cohesive-ends b vertically on the vertices on that column, and let one cohesive-end be distributed horizontally to the first column on that row. Distribute the cohesive-end a on tile t_3 horizontally to remaining incident edges. Note that the remaining vertices v_k for $k \in \{2, 3, 4, 6, 7, 8\}$ are associated to t_2 . Use Algorithm 2.7 in Phase 2 of Figure 4.7b to distribute the remaining cohesive-ends a and \hat{a} .

Example 4.11. Consider the 4×4 rook's graph. Let the colors black and red represent the bond-edge types a , b , respectively. The graph is built in two phases as in Figure 4.8. To complete the construction, superimpose Figure 4.8a and Figure 4.8b.

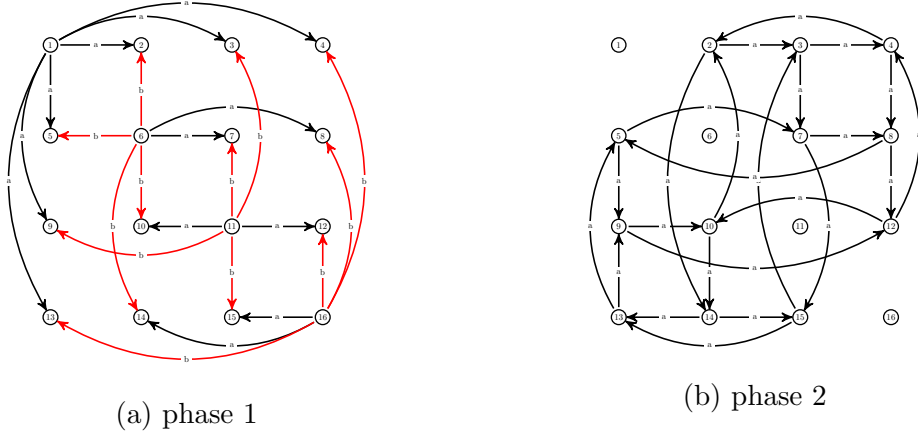


Figure 4.8: 4×4 rook's graph

Consider the following tiles: $t_1 = \{a^6\}$, $t_2 = \{a^2, \hat{a}^3, \hat{b}\}$, $t_3 = \{a^2, b^4\}$. Hence the pot $P = \{t_1, t_2, t_3\}$, has the associated construction matrix

$$M(P) = \left[\begin{array}{ccc|c} 6 & -1 & 2 & 0 \\ 0 & -1 & 4 & 0 \\ 1 & 1 & 1 & 1 \end{array} \right]$$

with solution $\langle \frac{1}{16}, \frac{3}{4}, \frac{3}{16} \rangle \in \mathcal{S}(P)$ and $m_p = 16$.

In Phase 1 of Figure 4.7a, let

$$\lambda(v_i) = \begin{cases} t_1 & \text{for } i \in \{1\} \\ t_3 & \text{for } i \in \{6, 11, 16\}. \end{cases}$$

Note that t_1 only has one choice for distributing its cohesive-ends. For tile t_3 distribute the cohesive-ends b vertically on the vertices on that column, and let one cohesive-end be distributed horizontally to the first column on that row. Distribute the cohesive-end a on tile t_3 horizontally to remaining incident edges. Note that the remaining vertices v_k for $k \notin \{1, 6, 11, 16\}$ are associated to t_2 . Use Algorithm 2.7 in Phase 2 of Figure 4.7b to distribute the remaining cohesive-ends a^2 and \hat{a}^2 .

The following theorem is a generalization of the preceding examples.

Theorem 4.12. *If G is an $n \times n$ rook's graph, then $B_2(G) = 2$ and $T_2(G) = 3$.*

Proof. According to Theorem 4.7, when $m \leq n$, $B_2(G) \geq 2$. Now it remains to be shown that $B_2(G) = 2$ and $T_2(G) = 3$. Let $P = \{t_1 = \{a^{2(n-1)}\}, t_2 = \{a^{n-2}, \hat{a}^{n-1}, \hat{b}\}, t_3 = \{a^{n-2}, b^n\}\}$. The associated construction matrix is

$$M(P) = \left[\begin{array}{ccc|c} 2(n-1) & -1 & n-2 & 0 \\ 0 & -1 & n & 0 \\ 1 & 1 & 1 & 1 \end{array} \right]$$

with solution $\langle \frac{1}{n^2}, \frac{n-1}{n}, \frac{n-1}{n^2} \rangle \in \mathcal{S}(P)$ and $m_p = n^2$ by Proposition 2.5.

To show that $G \in \mathcal{O}_{min}(P)$, consider the labeling on the vertices that has been shown in Figure 4.7 and Figure 4.8. Let $\lambda(v_1) = t_1$. There are $n-1$ vertices that remain along the main diagonal, let $\lambda(v_{1+k(n+1)}) = t_3$ for $k \in \{1, 2, \dots, n-1\}$. For the remaining vertices v_i such that $i \neq 1 + k(n+1)$ for $k \in \{0, 1, \dots, n-1\}$, let $\lambda(v_i) = t_2$. Then $G \in \mathcal{O}_{min}(P)$, $B_2(G) = 2$ and by construction along with applying Corollary 4.8, $T_2(G) = 3$. \square

Chapter 5

Conclusion

In conclusion, this paper explored the tile based DNA self-assembly of the rook's graph. Research of DNA self-assembly is about 35 years old [See82], and the rook's graph was studied for the first time in this thesis. The rook's graph is interesting because unlike previous classes of graphs studied in the context of DNA self-assembly, the rook's graph grows in two dimensions. Growing in two dimensions created several challenges in finding an assembly design. We have fully classified the rook's graph in Scenario 1. In Scenario 2, the $n \times n$ rook's graph, or the square case, was finished and we have partial results for the rectangular case. The hope was to use the fact that the $m \times n$ rook's graph is the Cartesian product $K_m \times K_n$ and to determine if in general, assembly designs can be found using this graph property. Although the assembly design for K_n worked for the $2 \times n$ rook's graph where n is odd in Scenario 2, it quickly failed after. Since it appears that Cartesian products of graphs do not immediately provide an assembly design, other design strategies had to be developed to finish $2 \times n$ graphs in Scenario 2. Scenario 3 is left as an open question due to the extra condition that non-isomorphic graphs cannot be constructed. Notice the pots described in Chapter 4 contain tiles with pairs of complimentary cohesive-ends. Such tiles can realize graphs with loops which is a quick way to determine if a pot realizes a non-isomorphic graph. Lastly, the general $m \times n$ case is still left as an open question under Scenario 2. Although, we have found lower bounds for $B_2(G)$ and $T_2(G)$, and we have examples of rook's graphs that achieve these bounds.

Bibliography

- [CZ12] G. Chartrand and P. Zhang. *A First Course in Graph Theory*. Dover books on mathematics. Dover Publications, 2012.
- [EMJP19] Joanna Ellis-Monaghan, Nataša Jonoska, and Greta Pangborn. Tile-based DNA nanostructures: mathematical design and problem encoding. In *Algebraic and combinatorial computational biology*, Math. Sci. Eng., pages 35–60. Academic Press, London, 2019.
- [EMP11] J. Ellis-Monaghan and G. Pangborn. Using DNA self-assembly design strategies to motivate graph theory concepts. *Math. Model. Nat. Phenom.*, 6(6):96–107, 2011.
- [EMPB⁺14] Joanna Ellis-Monaghan, Greta Pangborn, Laura Beaudin, David Miller, Nick Bruno, and Akie Hashimoto. Minimal tile and bond-edge types for self-assembling DNA graphs. In *Discrete and topological models in molecular biology*, Nat. Comput. Ser., pages 241–270. Springer, Heidelberg, 2014.
- [See82] Nadrian C. Seeman. Nucleic acid junctions and lattices. *Journal of Theoretical Biology*, 99(2):237 – 247, 1982.
- [See07] Nadrian C. Seeman. An overview of structural DNA nanotechnology. *Molecular Biotechnology*, 37(3):246, Jul 2007.